

RESEARCH

Open Access



# Impairment of Nrf2 signaling in the hippocampus of P301S tauopathy mice model aligns with the cognitive impairment and the associated neuroinflammation

Ahmed Sabry Mohamed<sup>1</sup>, Mahmoud ElKaffas<sup>2</sup>, Karim Metwally<sup>2</sup>, Mahmoud Abdelfattah<sup>2</sup>, Eslam Ashraf Elsery<sup>2</sup>, Ahmed Elshazly<sup>2</sup>, Hossam Eldin Gomaa<sup>2</sup>, Aziza Alsayed<sup>3</sup>, Sara El-Desouky<sup>3</sup>, Randa El-Gamal<sup>3,4,5,6</sup> and Sara Elfarrash<sup>3,7\*</sup>

## Abstract

Mice transgenic for human P301S tau protein exhibit many characteristics of the human tauopathies, including the formation of abundant hyperphosphorylated tau filaments, the associated neuroinflammation and disease phenotype. However, the exact underpinning mechanisms are still not fully addressed that hinder our understanding of the tauopathy diseases and the development of possible therapeutic targets. **Methods:** In the current study, hippocampus from three disease time points (2, 4 and 6 months) of P301S mice were further characterized in comparison to the age and sex matched control wild type mice (WT) that do not express the transgene. Different spectrum of hippocampal dependent cognitive tests, biochemical and pathological analysis were conducted to understand the disease progression and the associated changes in each stage. **Results:** Cognitive impairment was manifested as early as 2 months age, prior to the identification of tau aggregation and phosphorylation by immunostaining. P301S mice manifested an increased pro-inflammatory related changes at mRNA transcription level (IL-1b and IL17A) with the progression of the disease and when compared to the WT mice of the same age. Among the identified genes in the current study, the nuclear factor (erythroid-derived 2)-like 2 (Nrf2) genes expression that is considered as the master regulator of an endogenous inducible defense system was significantly impaired in P301S mice by 4 and 6 months when compared to healthy WT controls. A data that was also supported by the immunostaining of the serial brain sections including the both brain stem and hippocampus. The current result is suggesting that the downregulation of Nrf2 gene and the impaired Nrf2 dependent anti-inflammatory mechanisms in P301S mice brain is possibly contributing -among other factors- in the neuroinflammation and tauopathy, and that modulation of Nrf2 signaling impairments can be further investigated as a promising potential therapeutic target for tauopathy.

**Keywords** Tauopathy, Nrf2, P301S, Neuroinflammation, Memory impairment

\*Correspondence:  
Sara Elfarrash  
saraelfarrash@mans.edu.eg

Full list of author information is available at the end of the article



© The Author(s) 2024. **Open Access** This article is licensed under a Creative Commons Attribution-NonCommercial-NoDerivatives 4.0 International License, which permits any non-commercial use, sharing, distribution and reproduction in any medium or format, as long as you give appropriate credit to the original author(s) and the source, provide a link to the Creative Commons licence, and indicate if you modified the licensed material. You do not have permission under this licence to share adapted material derived from this article or parts of it. The images or other third party material in this article are included in the article's Creative Commons licence, unless indicated otherwise in a credit line to the material. If material is not included in the article's Creative Commons licence and your intended use is not permitted by statutory regulation or exceeds the permitted use, you will need to obtain permission directly from the copyright holder. To view a copy of this licence, visit <http://creativecommons.org/licenses/by-nc-nd/4.0/>.

## Introduction

The microtubule associated protein Tau is abundantly expressed in the central nervous system and has been widely recognized as being a fundamental protein in the assembling, stabilization and organization of the microtubules in axons [1]. Although the previous works failed to address the full physiological functions of Tau, the prominent filamentous Tau inclusions are heavily linked to the pathology of several neurodegenerative diseases collectively called tauopathy. This includes Alzheimer's disease (AD), sporadic frontotemporal dementia (FTDs), progressive supra nuclear palsy, Pick's disease, amyotrophic lateral sclerosis/parkinsonism-dementia complex, corticobasal degeneration and others [2–4]. Six isoforms of tau exist in a homeostatic balance in the adult neuronal cells [5] [6], and the mutations of the tau encoding gene (*MAPT*), altered isoform expression, hyperphosphorylation or conformational changes of the tau protein are all suggested to be actively contributing in the pathophysiology of different tauopathies [2] [7]. Subsequently, tau is consistently considered to be an attractive target for an effective therapy. To date, 67 different mutations in *MAPT* are identified in more than 100 families to cause frontotemporal dementia and parkinsonism linked to chromosome 17 (FTDP-17T) [8] establishing the concept that mutation of tau protein can in-part initiate a neurodegeneration, however there is little agreement on the possible mechanism. Although promising results were reported in experimental set ups, the lack of understanding of molecular mechanisms had hinder to translate those successes to the clinical trials.

Different mice models were developed in the last two decades, including P301S, that exhibit tau aggregation, post translational modification, in addition to glial activation, neuronal loss, and spectrum of different behavioral phenotype mimicking those observed in human AD and other tauopathies, and had been used extensively either to investigate the disease mechanism [9–14] or to try a tau-targeting therapeutic agents [15–18].

In addition to the protein aggregations, inflammation and oxidative damages have received a considerable interest as a potential candidate in the pathogenesis of neurodegenerative diseases, and many works have been devoted to study the inflammatory processes in neurodegenerative diseases, especially AD and PD [19–21]. The available data is suggesting that neuroinflammation and gliosis occur in early stages and also chronically persist throughout the disease progression, sparking the interest that inflammation can plays a fundamental role to exacerbate disease pathology, phenotype and neurodegeneration. Different attempts were also running to test anti-inflammatory drugs as a possible therapeutic option for AD, PD and associated tauopathy.

While the association of inflammation to tau pathology is already reported in both clinical and experimental studies using different models [10, 12, 14, 22–28], still there is no enough information regarding the molecular level alterations at the earlier stages, before the phenotype development or tau hyperphosphorylation. While this is not trivial, the identification of a potential candidate can accelerate our understanding and further be implemented for therapeutic potential and diagnostic potential as a possible biomarker. In the current study, we investigated the different inflammatory profiling of the widely used P301S tauopathy mice model, aligning the inflammatory changes at the RNA level, with the development and progression of the cognitive impairment and tau aggregation. Comparing the inflammation related profile at each time point of P301S compared to the age and sex matching -mutagen free- WT mice, had given us the insight for the possible impaired signals that can be contributing to the disease progression including Nrf2. The current data, while need a further investigation, demonstrated that inflammatory changes were not only closely associated to the phenotype and tau accumulation in P301S but also proceed the tau aggregation in some brain regions like hippocampus.

## Materials and methods

### Mice

This study protocol was approved by the Institutional research board Committee of Faculty of Medicine, Mansoura University (approval code: R.21.02.1220) and conformed complying with ARRIVE guidelines and were conducted in accordance with U.K. Animals ACT, 1986. Mice were bred and housed at temperature around 25°C in the animal facility of Medical Experimental Research Center (MERC), Faculty of Medicine, Mansoura University, Egypt. Mice were conditioned in standard cages (4 to 5 mice per cage) with an alternating 12 h light/dark cycle. Fed standard chow, and water was available *ad libitum*. Male Homozygous transgenic mice that overexpresses 0N4R human P301S mutant tau under the murine thyl promoter on a C57BL/6 background developed originally at Michel Goedert lab (University of Cambridge, UK) [29] were used and referred to as (P301S) throughout the manuscript. For the controls, an age and sex matching C57BL/6 purchased from MERC were used to ensure the genetic similarities between both groups, and are referred to as wild type (WT) throughout manuscript. The study included three time points (2, 4 and 6 months) where at each time point 9–11 P301S and WT mice were randomly allocated.

### Sample size

Sample size was calculated by using Power Analysis and Sample Size (PASS) Software (version 15, 2017). NCSS,

LLC. Kaysville, Utah, USA. Based on review of the literature, we hypothesized a factorial design with two factors; age with 3 levels (2, 4, and 6 months), and group with 2 levels (P301S and WT), i.e., 6 cells would have significant effects on behavioral and PCR parameters with large effects sizes (Cohen's  $f=0.4$ ). A total of 66 mice are required to provide 11 mice per cell. This design achieves 82% power when an F test is used to test age factor at a 5% significance level and the effect size is 0.400, achieves 89% power when an F test is used to test grouping factor at a 5% significance level and the effect size is 0.400, and achieves 82% power when an F test is used to test the Age\*group interaction at a 5% significance level and the effect size is 0.400.

### Behavioral tests

To evaluate the cognitive function and its temporal aspect, Morris water Maze (MWM) and T-maze were used, while Open field test was conducted to test the exploratory behavior and the motor performance.

### Morris water maze

To analyze the hippocampal dependent spatial learning and memory, the MWM was performed at 2, 4 and 6 months of age ( $n=11$  per group) in a 110 cm diameter cylindrical water basin with white painted walls as described originally with Richard Morris with slight modifications [30, 31]. A white painted platform was used and placed in the fixed place during the training days. Four bright and colorful signs were placed on the basin wall at each quadrant and the basin was not moved, nor the surroundings, during the test performance days to ensure a fixed proximal and distal cues. The test is composed of five days, pre-training (Day 0), training (Day 1, 2 and 3) and probe trial (Day 4). For pre-training, mice were left in the water to swim for 60 s freely with no platform. For training (Day 1, 2 and 3), mice were placed gently, facing the wall of the arena and let them swim to reach the platform that is submerged under the water level. Each mice get three trials daily, once from each quadrant apart from the one where the platform is placed. The interval between trials ranges between 4 and 9 min, depending on the performance of mice in each group to finalize all the mice. The time taken by each mouse to reach the platform is recorded and reported for each day as the latency period. Those mice that failed to reach the platform in the training days during the given 60 s were guided gently (without lifting them from the water) to the platform and left on the platform for 20 s, and the latency period for those mice are recorded as 60 s. Water was dyed using starch and not changed throughout the trial days, a part of cleaning up any floating poop pellets. During the probe trial (Day 4), the platform is removed, and each mouse is placed gently and let to swim freely for 60 s, the

time each mice spent in the quadrant that used to have the platform, are measured to address the preference to the correct quadrant. The temperature of the water was adjusted at 24 °C and mice were dried up after each trial and placed underneath the heat lamp at the end of each session to keep their body warm. The recorded videos of training and probe trial days were exported and analyzed using ANYMAZE software.

### Reward alteration in T-maze

To test the hippocampal dependent task with another procedure, a reward alteration test was as described earlier [32]. The test was carried out in total 5 days. The first day (Habituation) mice were just introduced to the T-maze arena and left to explore it freely with both arm gates are opened. The sweated condensed milk (Nestle) is introduced in the cage at this stage to ensure that the reward is palatable for the mice as a reward. For the training (Day 2,3 and 4), mice were trained to learn the alteration pattern of the reward in the T maze arena, non-sweated condensed milk is given in alternations in each arm. Ten trials were run for each mouse in a daily session for the 3 days. For the test day (Day 5), 10 trials were performed for each mice. Firstly, the mice are placed in the start arm, and forced to one arm with the reward in, by closing the sliding door of the opposite side, the mice are left to consume the reward (0.07 ml) and then left gently from the arena back to a cage. After completion of this stage for the all mice of the same group, each mice was gently placed to the starting point with the two sliding doors of both arms opened, but the reward is only placed at the opposite arm. The mice were allowed to consume the reward if entered the correct arm and counts as "Correct choice" while if the mice failed to alternate and entered the same arm, then it is counted as "Incorrect choice." The percentage of correct choices out of the 10 trials in the test days are calculated and reported for each mouse. The setting up of reward alteration are made randomly in advance for the all 10 trials, with the maximum of three consecutive arm of the same side to have the reward, as a precaution against temporary position habits developing.

### Open field

For the investigation of locomotor and exploratory activity, an open field test was done using a clear 40 cm × 40 cm box (Stoelting cat # 60,100) for 120 s in a dim light. A camera fixed at the roof of arena was used to record the session that is later analyzed using ANYMAZE software tracking system. The software divides the OF arena into a total of equal 16 squares, 4 (L) X 4 (W). The recorded videos were used to calculate the time spent in the peripheral zones i.e.: 12 squares in the perimeter of the arena, the central zones i.e.: total 4 squares in the

center of the arena, and the numbers of crossing lines to evaluate the locomotor function.

#### Mice sacrifice and sample collection

For sample collection, mice were injected with mixture of halothane and ketamine by an Intraperitoneal I injection, then after ensuring the anesthesia by checking the pedal reflex, the trans-cardiac perfusion were performed, either by using phosphate buffer saline (PBS) only (for samples collected for real time PCR), or PBS and followed with 10% formaline for samples collected for IHC were done. For RT-PCR, both hippocampi were extracted on cold petri dish and snap frozen immediately on dry ice and stored in  $-80^{\circ}\text{C}$  till the time of analysis. For mice allocated for IHC, mice brain were kept in 10% formaline following extraction for overnight at  $4^{\circ}\text{C}$ , to ensure proper fixation of brain tissue then proceed into paraffin blocks and kept at room temperature (RT) as described earlier [33].

#### mRNA quantification by real-time reverse transcription-PCR (qRT-PCR)

During processing, liquid nitrogen was used to homogenize hippocampi samples. To extract total cellular RNA, QIAzol (Qiagen, Germany) was used. Thermo Scientific NanoDrop One (USA) was used to check the yield of RNA and determine its concentration and purity. Using a Proflex Thermal Cycler (Applied Biosystems, USA) and SensiFASTTM cDNA synthesis Kit (Bioline, UK), first strand cDNA was synthesized from 1  $\mu\text{g}$  of RNA. Primers were annealed for 10 min at  $25^{\circ}\text{C}$ , reverse transcription took place for 15 min at  $42^{\circ}\text{C}$ , and inactivation took place for 5 min at  $85^{\circ}\text{C}$ .

Azure Cielo 6 (Azure, USA) real-time PCR was used to amplify cDNA templates. Ten microliters of SYBR green PCR Master Mix (Bioline, UK), 1  $\mu\text{l}$  cDNA template, 2  $\mu\text{l}$  (10 pmol/ $\mu\text{l}$ ) of gene primer, and 7  $\mu\text{l}$  of nuclease-free water made up the 20  $\mu\text{l}$  reaction volume. After adjusting the thermal profile for two minutes at  $95^{\circ}\text{C}$ , there were forty cycles: five seconds of denaturation at  $95^{\circ}\text{C}$ , followed by thirty seconds of annealing and extending at  $60^{\circ}\text{C}$ .

Some primers were newly designed using Primer3: <https://primer3.ut.ee/>. Version 4.1.0 Accessed on 5th February 2022, others were extracted from previous publications as demonstrated in (Supplementary Table 1). All primers' specificity was checked using NCBI Primer-BLAST program [<https://www.ncbi.nlm.nih.gov/tools/primer-blast/>] and purchased from Vivantis (Vivantis Technologies, Malaysia). Glyceraldehyde-3-phosphate dehydrogenase (GAPDH) was used as a reference gene. A melting curve analysis was performed to verify the PCR products' specificity. Primer sets were acquired as a Relative gene expression levels were represented as  $\Delta\text{Ct}=\text{Ct}$

$\text{target gene} - \text{Ct}_{\text{housekeeping gene}}$ ;  $2^{-\Delta\Delta\text{CT}}$  method was used to calculate the fold change in gene expression [34]. Calculations were done as two independent set ups, where the first considered the P301S mice of 2 month-age as a control group, then the genes fold change of the other P301S groups (4 and 6 months) were calculated versus it to evaluate the changes that occurs through the progression of the disease and age advancement of P301S. For the second set up, the wild type of each age was used as a control group for calculation of the genes fold change between the P301S mice group and the control WT of the same age.

- $\Delta\text{Ct1}$  (Control samples) =  $\text{Ct}(\text{target gene}) - \text{Ct}(\text{housekeeping gene})$
- $\Delta\text{Ct2}$  (Diseased samples) =  $\text{Ct}(\text{target gene}) - \text{Ct}(\text{housekeeping gene})$
- $\Delta\Delta\text{Ct} = \Delta\text{Ct2} - \Delta\text{Ct1}$
- Relative quantitation or fold change (RQ) =  $2^{-\Delta\Delta\text{Ct}}$

#### Immunohistochemistry and image quantification

The formalin fixed brains were dehydrated with ascending concentration of ethyl alcohol then cleared in xylene and embedded in the paraffin blocks till the time of analysis. Using a microtome (MicroTec cut 4050, Germany) brain was dissected into a serial 5  $\mu\text{m}$  sections and mounted on VWR® Superfrost® Plus Micro Slides. For Immunostaining, serially selected sections from P301S and WT groups were deparaffinized and rehydrated in xylene and an inverse dilution of alcohol then distilled water. For immune staining, sections underwent antigen retrieval in citrate buffer in microwave (set on max. power for 15 min) then left to cool in RT for 15 min. Followed with the routine quenching, sections were incubated for 20 min at RT with 0.5% Tritonx100/PBS for permeabilization with gentle shaking then 3% BSA/PBS was used as a blocking agent. Sections were then incubated with following primary antibodies: Antiphosphorylated Tau (Ser 202,Thr205) (AT8, cat# MN1020, Invitrogen 1:500) and (Thr212,Ser214) (AT100 cat#MN1060, Invitrogen 1:500), Anti-GFAP (D1F4Q) XP® Rabbit mAb #12,389, Cell Signaling Technology, 1:1000), NRF2 (Rabbit cat#A0674, ABclonal, 1:100) Primary antibody mixture made in 5% BSA were incubated for overnight in an in-house made humidity chamber with gentle shaking at  $4^{\circ}\text{C}$ . Sections were then washed for three times – 15 min each- using TBS/0.03% TritonX. The slides were stained with diaminobenzidine (DAB) (Mouse and rabbit HRP/DAB (ABC) detection IHC kit, ab64264, Abcam, UK) and the immunoreactivity was visualized as a brown color. Glial Fibrillary Acidic protein (GFAP) and Nrf2 stained sections were then counterstained with hematoxylin for 60 s. As negative control, sections from each group underwent



the same steps but with skipping the primary antibody and replacing it with the 5% BSA (Supplementary file 2). For imaging, Olympus CX41 was used to examine the sections and figures were photographed for quantification using a digital camera Olympus SC100. For quantification, FUJI was used, where seven non-overlapping random fields per section from each mouse were captured by x40 objective lens, tau reactive signals (AT8 and AT100), Nrf2 and GFAP signals were detected by counting the reactive cells then averaged per field for each section then for each animal in each group. Mean signal density was also calculated using FIJI for GFAP and Nrf2 staining as described earlier [35], briefly, in each image we implement the color deconvolution option, where the images are split into three channels and the DAB signal can be then quantified.

**Statistical analysis**

Statistical analysis was performed using GraphPad Prism 8.0.2. Data were tested for normality using the Shapiro–Wilks test. When comparing two groups (WT and P301S of same age) Student’s T test was used for the

normally-distributed data or Mann-Whitney U test for the non-normally distributed data. To compare more than two groups, one-way or repeated measures ANOVA followed by post hoc Tukey test was used when normally distributed or a non-parametric Kruskal–Wallis test followed with Dunn’s multiple comparison test for the non-normally distributed data. A *p*-value below 0.05 was considered significant where \**p*<0.05, \*\**p*<0.01, \*\*\**p*<0.001, \*\*\*\**p*<0.0001 except if otherwise mentioned in each figure legend.

**Results**

**P301s mice demonstrated a cognitive impairment as early as age of two months prior to the motor phenotype**

Morris water maze performance is linked to the spatial memory and long-term potentiation and therefore, used consistently for the assessment of the hippocampal dependent cognitive functions. P301S mice showed the impaired performance in the water maze as early as age of 2 months compared to the sex and age matching WT mice in finding the platform, demonstrated by taking a significantly longer latency time (Fig. 1a, b,c). The

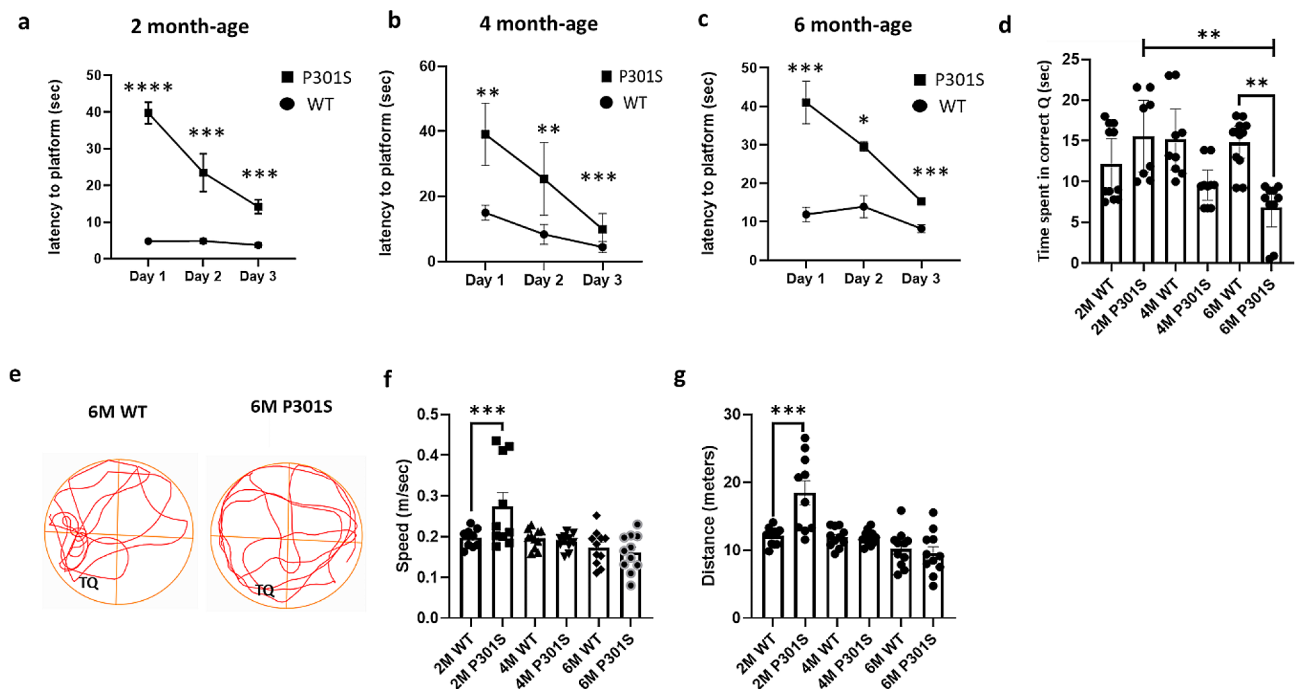


**Fig. 1** A progressive memory deficit of P301S in hippocampal dependent tasks using Morris Water Maze **a, b, c**: Dot chart demonstrating the latency time to reach platform (in seconds) in MWM from Day 1 to Day 3 showing a significant defect in the performance of P301S mice compared to the two, four and six months age matching WT mice. **d**: Bar chart demonstrates the mean of time spent in the target quadrant (TQ) during the probe trial of MWM, showing an age dependent significant impairment of retrieving the correct site of the platform for P301S mice in addition to the significant reduction in comparison to WT strains at 6 month-age. **e**: Representative tracking chart of ANYMAZE for 6 month-age WT and P301S mice showing the lack of preference to swim at the target quadrant (TQ) for P301S in comparison to WT mice. **f**: Bar graph representing the average swimming speed (m/sec) in MWM arena during the probe test day, showing a significant increase of the speed for 2 months P301S compared to the age matching WT and other groups. **g**: Bar graph representing the mean of total distance (m) covered by each group during the probe test in MWM arena, showing the significant hyperkinesia of 2 M P301S compared to other groups. Data are shown as mean ± SEM of 9–11 mice per group, and significance is tested with Students T test when comparing between P301S and WT strains of the same age, or using one way ANOVA test with post-hoc Tukey HSD test when comparing P301S at different age points or Kuskal-Wails followed with Dunn’s multiple comparison test. \**p*<0.05, \*\**p*<0.01, \*\*\**p*<0.001, \*\*\*\**p*<0.0001

reduction of the latency time seen by 3rd day compared to the 2nd and 1st day performance (p value=0.02 and 0.0002 respectively) suggest that P301S mice are still capable to learn the task till the age of 6 months, but still significantly taking more time compared to the WT group of the same age. During the probe test, the time spent in the correct quadrant (SW) was only significantly reduced by 6 months age group. At the age of 4 months, P301S mice showed tendency to spent less time at the correct quadrant compared to WT mice, however failed to reach the statistical significance (Fig. 1d, e). P301S mice swam a longer total distance and with higher speed in the maze during the probe test compared to the 2 month-age WT, but no difference regarding the distance or swimming speed was detected at the 4 or 6 months ages, suggesting that the motor function of P301S were not affected at this disease stage. (Fig. 1f, g). In T maze test, mice of all age groups were taught to choose the alternated arm that contains a reward, 4 and 6 month-age P301S failed significantly to make correct choices during the test day compared to the control WT mice (Fig. 2,a).

For the assessment of motor functions and the exploration behavior, mice were placed gently to move freely using open field test arena. The motor impairment was detected as a reduction of total numbers of crossed lines by four and six months age for P301S mice (Fig. 2,b). Although no differences were detected in the time spent in the periphery nor the center of the arena in 2 and 4 months, P301S mice of 6 months-age, spent more time in the central zones than peripheral zones compared to WT of the same age (Fig. 2, c, d). This was correlated to the immobility of the majority of mice in this group identified through the examiners and tracking data, suggesting a motor impairment developed at this stage for P301S, or at least the unwillingness of mice to move during the test.

#### **Tau aggregation and phosphorylation start by four month-age and significantly increases by 6 months in the P301S mice with regional variations**

Phosphorylation of tau has been used widely to identify the pathologically aggregated tau where different phosphorylation sites were reported to be identified at the pathological aggregated forms of the Tau proteins. Immunostaining of P301S brain sections revealed that accumulation of AT8 and AT100 reactive phosphorylated tau are detected by four months-age with a significant increase in six months age P301S (Fig. 3). No Tau signals were detected neither in the 2 month stage of P301S nor the all tested points of WT sytatin (data not shown). Majority of tau aggregates were found in the brain stem (Fig. 3a, b) and show a significant increase with disease progression (Fig. 3, c, d) while tau aggregation at the hippocampus were only identified sparsely later at 6 months (Fig. 3e, f).

#### **Alteration of the inflammation related genes foreruns the tau phosphorylation in the hippocampus of P301S brain**

Neuroinflammation is closely associated with different neurodegenerative diseases including AD. Many studies suggested that tau aggregation can either initiates or causes a disruption in redox balance leading to an imbalance between anti and pro-inflammatory phenotypes of glia cells. To assess the changes of inflammation related genes of hippocampus through the disease progression in P301S, hippocampi from each time-point were analyzed for evaluation of their relative expression level by qPCR. *Nrf2* and *HOX1* that are considered as a cytoprotective genes were significantly down regulated with progression of the disease at 4 and 6 months (Fig. 4a, b), while *IL-1 $\beta$* , *IL-17 A*, *iNos*, *TNF- $\alpha$*  that considered pro-inflammatory cytokines were significantly increased (Fig. 4d, f, h, i) or showed a tendency to decreased as in *IL-6* (Fig. 4, e). Other showed no significant alterations like *Iba1* and *IL-10* with disease progression (Fig. 4, c, g). We also looked at apoptosis related genes and while *Bax* were increased, none of *Bcl2* nor *Caspase3* showed a significant alteration at the studied time points (Fig. 4j, k, l).

#### **P301S hippocampi are more vulnerable for inflammatory insults than the age matching WT mice**

To study the effect of transgene on the inflammatory related genes expression, we compared the qPCR data of P301S and WT of same age points. *Nrf2* gene showed a striking reduction observed at 4 months with further reduction at 6 months compared to the age matching WT mice. This however, comes after a surprising initial elevation at 2 months that failed shortly to reach a statistical significance at p value of 0.059 (Fig. 5,a). This can suggest the possible failure of cytoprotective machinery in P301S in line with tau aggregation, that comes at later stages after the failure to overcome the homeostasis imbalance at the earlier age points where inflammatory changes were already started. *HMOX1*, the downstream gene of *Nrf2*, that suggested to have an anti-inflammatory and neuroprotective effect showed a significant reduction compared to WT mice in line with the reduction of *Nrf2* in P301S in comparison to WT (Fig. 5, b). Pro-inflammatory cytokines like *IL-1 $\beta$*  and *IL-17 A* mRNA expression level was found to be higher in P301S manifested at 6 months age but not *IL-6* (Fig. 5,d, e,f). *IL-10* mRNA expression level, that is considered to be anti-inflammatory cytokine were found to be significantly reduced at the age of 2 months in P301S, suggesting the P301S can be more prone for inflammation at this early time point (Fig. 5,g). Other genes (*Iba1*, *iNOS* and *TNF- $\alpha$* ) didn't show significant alteration in our hands compared to the age matching WT (Fig. 5c, h, i). Out of the tested apoptosis related genes, only *Bax* showed significant increase compared to WT mice at 6 months (Fig. 5,

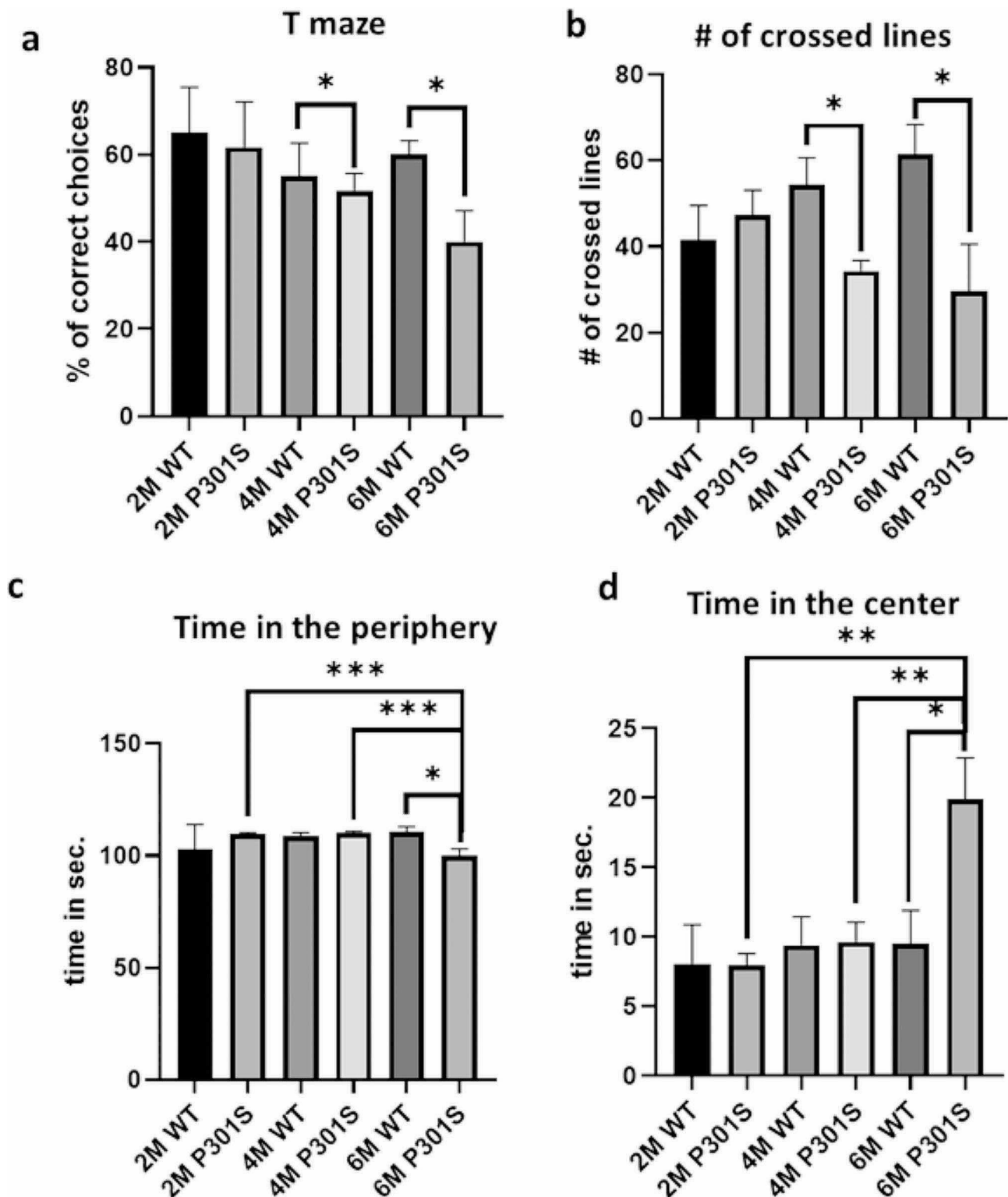


**Fig. 2** P301S mice demonstrated a behavioral and motor deficit identified by using T maze Reward alteration test and Open field test. **(a)** Bar graph showing the mean percentage of the correct choices (out of 10 trial) made by each group in Reward based T-maze test, showing the reduction of successful alteration in 4 and 6 months P301S mice. **(b)** Bar chart showing the mean of number of crossed lines during the open field test session suggesting the motor impairment in P301S mice at age of 4 and 6 months. **c, d.** Bar chart showing the mean of time spent in the peripheral and central zone of Open field test arena (in seconds) out of 120 s session. Data are shown as mean  $\pm$  SEM of 9–11 mice per group, and significance is tested with Students T test when comparing between P301S and WT strains of the same age, or using one way ANOVA test with post-hoc Tukey HSD test when comparing P301S at different age points. \*  $p < 0.05$ , \*\*  $p < 0.01$ , \*\*\*  $p < 0.001$

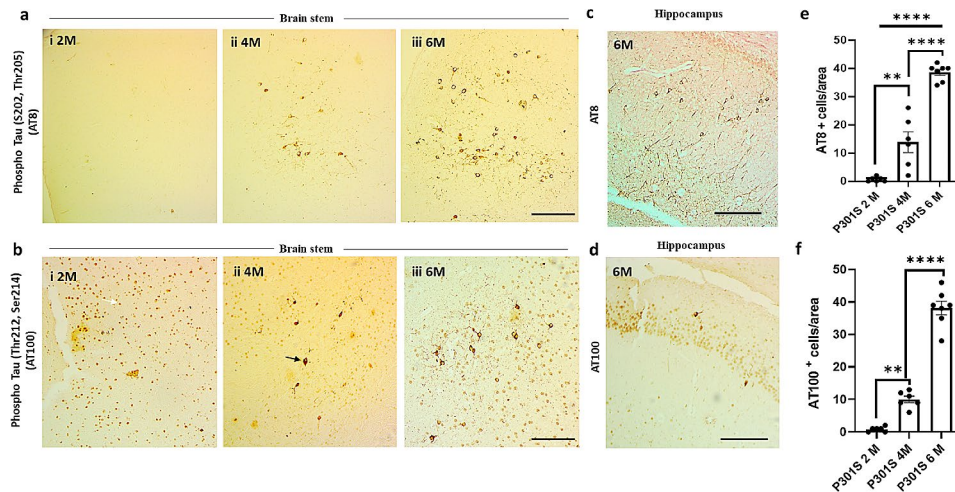


**Fig. 3** Immunostaining of brain tissue shows a progressive accumulation of phosphorylated tau protein. a and b. Representative image of brain stem from P301S mice stained with (a) AT8 and (b) AT100 antibody shows i: No AT8 or AT100 tau signals were detected at brain of 2 months age P301S. ii and iii: show progressive accumulation of AT8 and AT100 reactive tau in P301S mice at 4 and 6 months respectively. c and d: Representative image from the hippocampus showing AT8 (c) and AT100 (d) reactive tau aggregates appears at 6 months P301S mice. Black arrows for tau apoepecific signals, white arrow for nonspecific nuclear signal detected by AT100. (e) and (f): Bar graphs showing quantification of the AT8 and AT100 immunoreactive tau at the three age points represented as mean +/- SEM of brain sections from 4–6 mice per group. P value is tested by One-way ANOVA test followed with post hoc Tukey test where \*\*  $p < 0.01$  and \*\*\*\*  $p < 0.0001$ . Scale bars = 100  $\mu\text{m}$

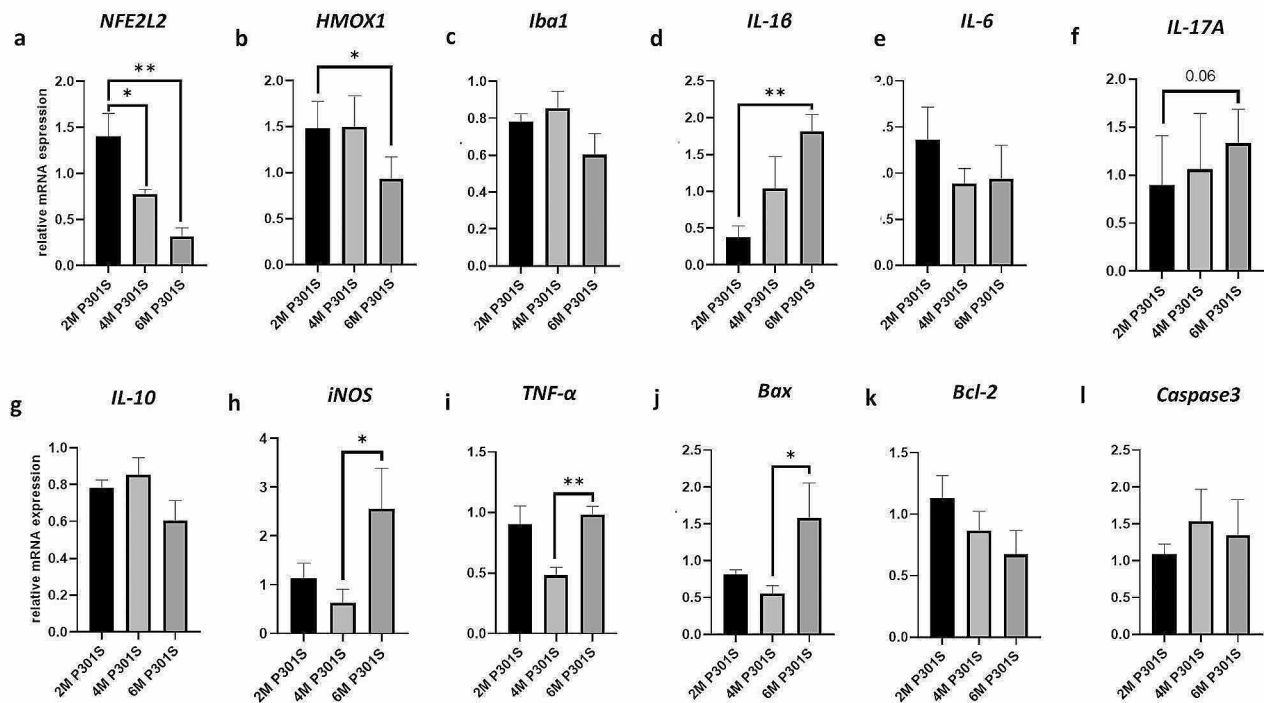


**Fig. 4** Relative mRNA expression level of the inflammation and cell death associated genes show a significant alteration through the tauopathy progression in P301S mice. The relative mRNA expression levels are presented by bar graphs for (a) *NFE2L2* (b) *HMOX1*, (c) *Iba1*, (d) *IL-1 $\beta$* , (e) *IL-6*, (f) *IL-17A* (g) *IL-10*, (h) *iNOS*, (i) *TNF- $\alpha$* , (j) *Bax*, (k) *Bcl-2* and (l) *Caspase3*. Data are shown as mean +/- SEM of 4–6 mice per group, and significance is tested with One-way ANOVA test followed with post hoc Tukey test when a significance between tested groups were detected. \*  $p < 0.05$ , \*\*  $p < 0.01$



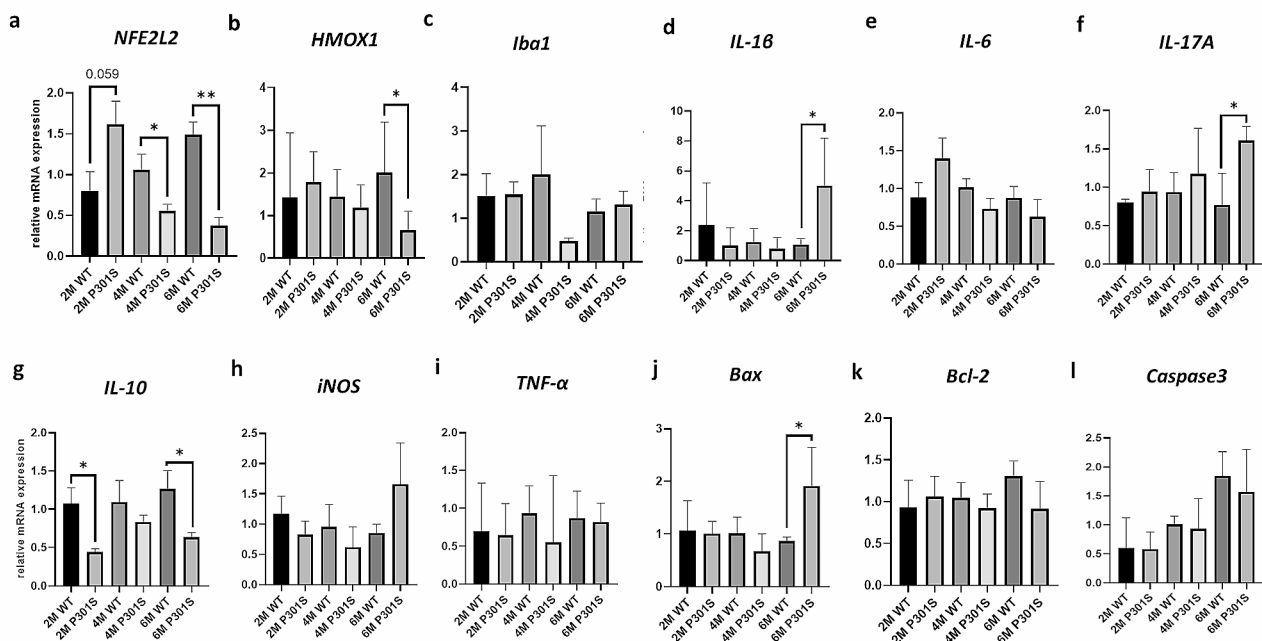


**Fig. 5** Relative mRNA expression level of Inflammation and cell death associated genes of P301S mice show distinct pattern compared to their age matching wild type controls. The relative mRNA expression levels are presented by bar graphs for (a) *NFE2L2* showing an increased expression level at 2 month age of P301S compared to WT that is followed with reduction at 4 and 6 months age (b) *HMOX1* expression is significantly reduced compared to WT at 6 months (c) *Iba1*, (d) *IL-1β* showed a high expression at 6 month, (e) *IL-6*, (f) *IL-17A* (g) *IL-10* showed a significant reduction at 2 and 6 months groups, (h) *iNOS*, (i) *TNF-α*, (j) *Bax*, (k) *Bcl-2* and (l) *Caspase 3*. Data are shown as mean  $\pm$  SEM of 4–6 mice per group, and significance is tested with One-way ANOVA test followed with post hoc Tukey test when significance between tested groups were detected. \*  $p < 0.05$ , \*\*  $p < 0.01$ . x-axis shows the relative mRNA expression in all graphs

j), but no significant changes were detected at the level of *Bcl2* or *caspase3* (Fig. 5, k and l).

#### Astrogliosis fore-run the tau aggregation in P301S mice

Immunostaining of P301S mice and the age matching controls with GFAP showed an evident astrogliosis, where GFAP reactive cell numbers and their density were both significantly increased as earlier as 2 months age group compared to WT, and increased progressively in P301S mice with disease progression. The astrogliosis was detected at both brain stem (with the heavy tau phosphorylation) and also the hippocampus (where tau were less abundant). Meanwhile the age progression showed no difference in GFAP expression in the WT controls (Fig. 6a-d).

#### Reduced Nrf2 expression in the brain of P301S, goes in parallel to the tau aggregation and the increased astrogliosis

To evaluate the expression level of total Nrf2 at each P301S disease time point, serial brain sections were stained with anti Nrf2 antibody. Nrf2 immunoreactive cell numbers and their density were reduced significantly, with sparse nuclear translocation in the P301S mice at 4- and 6-months ages in parallel to the aggregation of

tau phosphorylation and increased astrogliosis. While at 2 months point, there were an increased Nrf2 expression observed at some sections suggestion that Nrf2 can be increasing at the earlier stages of the tauopathy mice model in line with qPCR data, but it failed to reach a statistical significance. (Fig. 6e-h).

#### Discussion

In the current study, we validated and characterized the inflammatory profile of P301S tauopathy mice model that had been used constantly in the field but brought for the very first time to our lab in MERC, Mansoura University, Egypt. P301S strain is reported to show an increased insoluble tau from starting around 5 months, in addition to signs of inflammatory response [10]. The current study investigated the earlier stages of tauopathy progression in P301S mice model, before the initiation of tau phosphorylation, aggregation or neuronal loss.

Through examining the three different time points (2, 4, and 6 months) of disease progression, our data revealed that P301S strain shows an obvious hippocampal dependent cognitive impairment in both Morris water maze and the reward alteration T maze tests by 4 and 6 months. P301S mice were still able to learn the task in MWM test, noted by the reduction of latency period

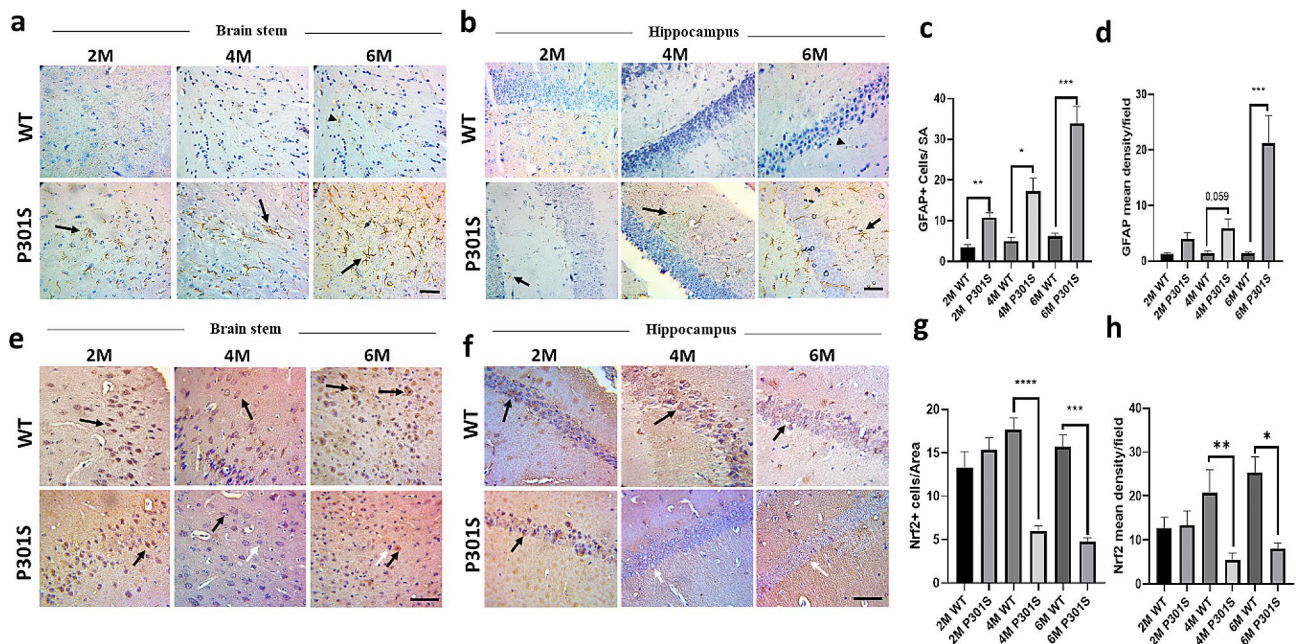


**Fig. 6** Immunostaining of brain sections from P301S and WT mice demonstrates a significant increase of astrogliosis and reduction of Nrf2 through the progression of tauopathy. **a** and **b** : Representative images of GFAP staining from WT mice (upper panel) and P301S (lower panel) from brain stem (**a**) and hippocampus (**b**) showing the early accumulation of GFAP reactive astrocytes by 2 month age for P301S mice and shows a progressive increase at 4 and 6 months. GFAP signals from P301S manifest a bold cytoplasmic processes (arrow) while a few resting astrocytes with fine cytoplasmic processes and mild expression are shown from the brain sections of WT mice (arrow heads). Scale bar = 20  $\mu$ m. **c** and **d**: Bar graphs representing the quantitative analysis of mean of GFAP<sup>+</sup> cell counts per field from all the imaged brain sections for 2, 4 and 6 months P301S and WT mice (**c**) and GFAP signals mean density (**d**). **e** and **f**: Show the representative figures from Nrf2 staining of brain section of WT mice (upper panel) and P301S (lower panel) from brain stem (**e**) and hippocampus (**f**), showing a reduction of Nrf2 expression with the progression of the tauopathy in P301S compared to sections from WT mice at 4 and 6 months. The perinuclear staining of Nrf2 identified in the brain sections from WT or the early stages of P301S (arrow), is significantly reduced at 4 and 6 months P301S. **g** and **h**: Bar graphs representing the quantitative analysis of mean of Nrf2+ cell counts per field (**g**) and Nrf2 signals mean density per examined field from all the imaged brain section (**h**). Data for all graphs are expressed as mean  $\pm$  SEM of brain sections from 5 to 6 mice. P value is tested by using Student's T test to compare between two strains of the same age group. p values throughout the figure are expressed as follow: \*  $p < 0.05$ , \*\*  $p < 0.01$ , \*\*\*  $p < 0.001$  and \*\*\*\*  $p < 0.0001$

during the training days of MWM, still, the latency the time required to reach the platform was significantly longer throughout the test. In addition, the spatial recalling of the “correct quadrant” during the probe test was defective significantly compared to the age matched WT controls at 6 months age. Evaluation of swimming speed and distances showed no significant reduction at tested time points for P301S mice compared to WT, suggesting that the reduction of time spent in the correct quadrant is mostly due to the cognitive impairment rather than a significant inability of the mice to swim at those disease stages in the water maze. T maze tests results showed the impaired ability to recall the alteration of reward place by 4 months and 6 months age groups in-line with results of MWM. In OF test, an initial increase in the speed and covered distance at 2 months age group were identified, in line with the earlier reported data by other groups at this age groups [10]. The motor impairment demonstrated by reduction of numbers of crossed lines and reduced covered distance in OF test, in contrast to the non affected swimming distance and speed

of P301S mice to perform in MWM, is mostly due to the lack of aversive stimuli in the OF test in contrast to the MWM that force mice to swim for a sake of dry platform. The motor impairment of P301S at this stage has been reported earlier due to the affection of the anterior horn cells with tau overexpression and aggregation [23].

For assessment of tau phosphorylation in P301S brain at the assigned time points, antibodies targeting different phosphorylation sites that are reported to be associated with pathological aggregation were used (S202, Thr205, Thr212 and Ser214). Our data revealed a progressive accumulation of phosphorylated Tau at different brain regions mainly the hindbrain and to less extent at the hippocampus of P301S mice starts only at 4 months and increase progressively by 6 months. No phosphorylated tau was detected at 2 months aged P301S. This goes in line with most of the studies at our target points [10, 12, 14, 27, 36]. While the cognitive impairment progression during the probe test and T maze goes in consistence with the accumulation of tau in P301S mice, an earlier behavioral phenotype detected including the training

stages of MWM, the hyper activity detected in OF and the observation that tau accumulation is not the most abundant in the hippocampus, are suggesting that part of the identified behavioral phenotypes are not solely Tau dependent and other changes can be contributing actively at the earlier points of the disease.

Many evidences suggest that neuroinflammation is a fundamental component of different neurodegenerative diseases such as AD, PD, and ALS [20, 21, 37–43]. Inflammatory changes were also reported for patients with FTD [26], and have been consistently reproduced in mice models of tauopathy [10, 24, 27]. To depict the relation between the detected early hippocampus dependent behavioral phenotype, tau aggregation process and the neuroinflammation, hippocampi from the each time points were isolated and different panels of inflammation dependent genes were evaluated in the current study. Current data demonstrated the over expression of pro inflammatory genes like *IL-1b*, *IL-17 A* and *iNOS*, suggesting the upper hand of inflammation with the disease progression, with reduction of anti inflammatory machinery like Nrf<sub>2</sub> and Hox1. On comparing qPCR data of P301S with the control B6 mice, revealed that P301S strain is more vulnerable for inflammatory changes than WT mice due to the deficient expression of cytoprotective genes like Nrf<sub>2</sub> and its downstream genes *Hox1*, detected significantly at 4- and 6-months age groups. Nrf<sub>2</sub> is a transcription factor that its main function is to protect cells from oxidative stress, thus maintaining the cells' redox homeostasis. Different studies had demonstrated Nrf<sub>2</sub> reduction in normal aging and diseases like AD and PD, in both experimental and clinical set ups [44–48]. In addition, studies showed earlier that knocking out (*Nrf2KO*) in mice models reported to develop a cognitive impairment, mimicking the aging phenotype and exacerbates the AD-like symptoms [49, 50]. This is consistent with our data that shows that Nrf<sub>2</sub> reduction is manifested in the hippocampus of P301S mice as early as 4 months and the level reduces more progressively by 6 months, which aligns with the further progression of cognitive impairment and tau aggregates accumulation in P301S brain. This also correlate favorably with other signs of inflammation observed with the qPCR data (including elevation of *IL-1β*, *IL-17 A* and *TNFα* and reduction of *IL-10*) and the evident astrogliosis detected by IHC, that collectively suggesting that Nrf<sub>2</sub> reduction in the hippocampus of P301S mice allows the oxidative stress to go unmitigated and drive the disease phenotype. Additionally, we need to emphasize on the effect of aging, and how the defective anti-inflammatory genes in P301S can be compromising the efficiency of handling the age-associated inflammatory insults, considering the progressive nature of tau accumulation and the pro-inflammatory profile observed. It's also noteworthy that

the downstream gene of Nrf<sub>2</sub>, *HMox1*, was also found to be reduced by the time of tau aggregation at 6 months and significantly lower than the expression level in the age matching WT mice. The suggested role of *HMox1* as an anti-inflammatory and neuroprotective transcription factor [51–53] elaborates on our conclusions that P301S mice is more vulnerable than WT mice for neuroinflammation at the studied disease stage.

Contrarily to the advanced stages of the disease, Nrf<sub>2</sub> expression at 2 months P301S group showed a consistent tendency to increase when compared to the WT control. Although it came short for a statistical significance, relative mRNA expression was increased compared to control 2 month with (p value of 0.059), also this initial increase was complemented with IHC data of brain sections stained with anti Nrf<sub>2</sub> that showed an initial increase in few sections at 2 months P301S. Although it should be further investigated and handled with caution till supported with more data at other time points like 1 and 3 months P301S, the current data suggests that Nrf<sub>2</sub> level elevation can be an initial attempt to overcome the cellular imbalance at 2 months P301S age group, prior to tau aggregation in accordance with the astrogliosis. This necessarily need not to be overlooked, because the possible hypothesis is that an initial attempt to the cytoprotective mechanisms of the cells come at early stages of the disease and forerun the Tau protein aggregation, as an attempt for boosting neuronal anti-oxidant response. Although some available data in literatures suggest that acute inflammatory responses induced by protein aggregation or an induced oxidative stresses in neurons or microglia cell lines can be Nrf<sub>2</sub> independent [54, 55] further experiments using a validated animal models and human samples can help to genuinely understand the molecular responses at the earlier stages of the disease. In spite the important finding that relate the inflammatory responses to tau aggregation, we are aware that our study also have number of limitations. A further characterization of Nrf<sub>2</sub> in specific cells, including neuron and glia cells can be fundamental to understand the pivotal role played by Nrf<sub>2</sub> signaling in auxopathies, also implementing further experiments to include female P301S is also essential, to understand the effect of sex dimorphism as reported earlier by other groups in P301S. Future experiments that include more time points can help to understand the role played via Nrf<sub>2</sub> modulation throughout the tauopathy progression and can pave the way for suggesting Nrf<sub>2</sub> activators as a promising approach to mitigate neurodegeneration in tauopathy and other related neurodegenerative diseases.

## Conclusion

Increasing evidences are suggesting inflammation is playing a fundamental role in pathogenesis of neurodegenerative diseases including tauopathy. In this study, we have demonstrated that the inflammatory modulation in hippocampus is closely associated to the phenotype development and progression. A possible role of specific genes like *Nrf2* is strongly suggested where a further experiment including more time points can help to more clearly understand the possible role played as a master of neuromodulation as described earlier. We conclude that the consistent reduction of *Nrf2* expression is actively contributing the tauopathy disease progression and phenotypes in P301S, while it is also important to further investigate the possible increased of *Nrf2* at the earlier stages that can be a good candidate for an earlier intervention or biomarker.

## Abbreviations

AD	Alzheimer's disease
ALS	Amylotrophic lateral sclerosis
BSA	Bovine serum albumin
FTD	Fronto-temporal dementia
FTD-17T	Fronto-temporal dementia with Parkinsonism
IHC	Immunohistochemistry
KO	Knock out
MATP	Microtubule Associated Tau protein
MWM	Morris water maze
Nrf2	Nuclear factor erythroid 2-related factor 2
OF	Open field
PBS	Phosphate buffer saline
PBS	Phosphate buffer saline
PD	Parkinson's disease
RT	Room temperature
SW	South west
WT	Wild type

## Supplementary Information

The online version contains supplementary material available at <https://doi.org/10.1186/s12950-024-00396-9>.

Supplementary Material 1

## Acknowledgements

The authors would like to thank Dr. Hend Hassan, Department of anatomy, Mansoura University for her assistance with the imaging and the Open access funding provided by The Science, Technology & Innovation Funding Authority (STDF) in cooperation with The Egyptian Knowledge Bank (EKB).

## Author contributions

SE, RE, AS, MK designed the study. AS, MK, KM, MA, EA, AH, HE and RE generated and analyzed the behavioral and real-time PCR data. SD and AA generated and analyzed histopathology data. SE and RE wrote the manuscript draft and all of authors critically revised it. All authors read and approved the final version of the manuscript.

## Funding

This work was funded by Mansoura Manchester Programme for Medical Education (MMPME) Faculty of Medicine, Mansoura University, Egypt (cycle #1) to AS, STDF grant #22990 and Mansoura University competitive grant (Mu-Med-20-31) to SE. Real time PCR experiments set up was part of STDF grant #41873 to SE and RG.

## Data availability

No datasets were generated or analysed during the current study.

## Declarations

### Ethical approval

The experimental animal protocol of this work was approved by the Institutional research board Committee of Faculty of Medicine, Mansoura University (approval code: R.21.02.1220) and conformed complying with ARRIVE guidelines and were conducted in accordance with U.K. Animals ACT, 1986.

### Competing interests

The authors declare no competing interests.

### Author details

<sup>1</sup>Program of Medicine, Faculty of Medicine, Mansoura University, Mansoura 35516, Egypt

<sup>2</sup>Mansoura Manchester Medical Program, Faculty of Medicine, Mansoura University, Mansoura 35516, Egypt

<sup>3</sup>Medical Experimental Research Center (MERC), Faculty of Medicine, Mansoura University, Mansoura 35516, Egypt

<sup>4</sup>Department of Medical Biochemistry & Molecular Biology, Faculty of Medicine, Mansoura University, Mansoura 35516, Egypt

<sup>5</sup>Department of Medical Biochemistry, Faculty of Medicine, Horus University, New Damietta, Egypt

<sup>6</sup>Department of Medical Biochemistry, Faculty of Medicine, New Mansoura University, Mansoura, Egypt

<sup>7</sup>Department of Medical Physiology, Faculty of Medicine, Mansoura University, Mansoura 35516, Egypt

Received: 3 January 2024 / Accepted: 24 May 2024

Published online: 06 August 2024

## References

1. Harada A, Oguchi K, Okabe S, Kuno J, Terada S, Ohshima T, et al. Altered microtubule organization in small-calibre axons of mice lacking tau protein. *Nature*. 1994;369:488–91.
2. Spillantini MG, Goedert M. Tau protein pathology in neurodegenerative diseases. *Trends Neurosci*. 1998. p. 428–33.
3. Tolnay M, Probst A. Tau protein pathology in Alzheimer's disease and related disorders. *Neuropathol Appl Neurobiol*. 1999. p. 171–87.
4. Goedert M. Filamentous nerve cell inclusions in neurodegenerative diseases: tauopathies and  $\alpha$ -synucleinopathies. *Philos Trans R Soc B Biol Sci*. 1999;354:1101–18.
5. Goedert M, Spillantini MG, Jakes R, Rutherford D, Crowther RA. Multiple isoforms of human microtubule-associated protein tau: sequences and localization in neurofibrillary tangles of Alzheimer's disease. *Neuron*. 1989;3:519–26.
6. Buée L, Bussièrè T, Buée-Scherrer V, Delacourte A, Hof PR. Tau protein isoforms, phosphorylation and role in neurodegenerative disorders. *Brain Res Rev*. 2000. p. 95–130.
7. Lee VMY, Goedert M, Trojanowski JQ. Neurodegenerative tauopathies. *Annu Rev Neurosci*. 2001. p. 1121–59.
8. Strang KH, Golde TE, Giasson BI. MAPT mutations, tauopathy, and mechanisms of neurodegeneration. *Lab Invest*. 2019. p. 912–28.
9. Ramsden M, Kotilinek L, Forster C, Paulson J, McGowan E, SantaCruz K, et al. Age-dependent neurofibrillary tangle formation, neuron loss, and memory impairment in a mouse model of human tauopathy (P301L). *J Neurosci*. 2005;25:10637–47.
10. Scattoni ML, Gasparini L, Alleva E, Goedert M, Calamandrei G, Spillantini MG. Early behavioural markers of disease in P301S tau transgenic mice. *Behav Brain Res*. 2010;208:250–7.
11. Spiess TL, Orne JD, SantaCruz K, Pitstick R, Carlson GA, Ashe KH, et al. Region-specific dissociation of neuronal loss and neurofibrillary pathology in a mouse model of tauopathy. *Am J Pathol*. 2006;168:1598–607.
12. Xu H, Rösler TW, Carlsson T, de Andrade A, Bruch J, Höllerhage M, et al. Memory deficits correlate with tau and spine pathology in P301S MAPT transgenic mice. *Neuropathol Appl Neurobiol*. 2014;40:833–43.



13. Yue M, Hanna A, Wilson J, Roder H, Janus C. Sex difference in pathology and memory decline in rTg4510 mouse model of tauopathy. *Neurobiol Aging*. 2011;32:590–603.
14. Wenger K, Viode A, Schlaffner CN, van Zalm P, Cheng L, Dellovade T et al. Common mouse models of tauopathy reflect early but not late human disease. *Mol Neurodegener*. 2023;18.
15. Santacruz K, Lewis J, Spire T, Paulson J, Kotilinek L, Ingelsson M, et al. Medicine: tau suppression in a neurodegenerative mouse model improves memory function. *Sci (80-)*. 2005;309:476–81.
16. Hampton DW, Webber DJ, Bilican B, Goedert M, Spillantini MG, Chandran S. Cell-mediated neuroprotection in a mouse model of human tauopathy. *J Neurosci*. 2010;30:9973–83.
17. Salama M, Elhussiny M, Magdy A, Omran AG, Alsayed A, Ashry R, et al. Dual mTORC1/mTORC2 blocker as a possible therapy for tauopathy in cellular model. *Metab Brain Dis*. 2018;33:583–7.
18. Salama M, El-Desouky S, Alsayed A, El-Hussiny M, Magdy K, Fekry E, et al. siRNA blocking of mammalian target of Rapamycin (mTOR) attenuates Pathology in Annonacin-Induced Tauopathy in mice. *Neurotox Res*. 2019;35:987–92.
19. Kwon HS, Koh SH. Neuroinflammation in neurodegenerative disorders: the roles of microglia and astrocytes. *Transl Neurodegener*. 2020.
20. Tansey MG, Wallings RL, Houser MC, Herrick MK, Keating CE, Joers V. Inflammation and immune dysfunction in Parkinson disease. *Nat Rev Immunol*. 2022. p. 657–73.
21. Zhang W, Xiao D, Mao Q, Xia H. Role of neuroinflammation in neurodegeneration development. *Signal Transduct Target Ther*. 2023.
22. Sun Y, Guo Y, Feng X, Jia M, Ai N, Dong Y et al. The behavioural and neuropathologic sexual dimorphism and absence of MIP-3α in tau P301S mouse model of Alzheimer's disease. *J Neuroinflammation*. 2020;17.
23. Macdonald JA, Bronner IF, Drynan L, Fan J, Curry A, Fraser G, et al. Assembly of transgenic human P301S tau is necessary for neurodegeneration in murine spinal cord. *Acta Neuropathol Commun*. 2019;7:44.
24. Perea JR, García E, Vallés-Saiz L, Cuadros R, Hernández F, Bolós M et al. p38 activation occurs mainly in microglia in the P301S tauopathy mouse model. *Sci Rep*. 2022;12.
25. Xie J, Zhang Y, Li S, Wei H, Yu H, Zhou Q et al. P301S-hTau acetylates KEAP1 to trigger synaptic toxicity via inhibiting NRF2/ARE pathway: a novel mechanism underlying Htau-induced synaptic toxicities. *Clin Transl Med*. 2022;12.
26. Bellucci A, Bugiani O, Ghetti B, Spillantini MG. Presence of reactive microglia and neuroinflammatory mediators in a case of frontotemporal dementia with P301S mutation. *Neurodegener Dis*. 2011;8:221–9.
27. Bellucci A, Westwood AJ, Ingram E, Casamenti F, Goedert M, Spillantini MG. Induction of inflammatory mediators and microglial activation in mice transgenic for mutant human P301S tau protein. *Am J Pathol*. 2004;165:1643–52.
28. Bruch J, Xu H, Rösler TW, De Andrade A, Kuhn P, Lichtenthaler SF, et al. PERK activation mitigates tau pathology in vitro and in vivo. *EMBO Mol Med*. 2017;9:371–84.
29. Allen B, Ingram E, Takao M, Smith MJ, Jakes R, Virdee K, et al. Abundant tau filaments and nonapoptotic neurodegeneration in transgenic mice expressing human P301S tau protein. *J Neurosci*. 2002;22:9340–51.
30. Morris R. Developments of a water-maze procedure for studying spatial learning in the rat. *J Neurosci Methods*. 1984;11:47–60.
31. Morris RGM, Garrud P, Rawlins JNP, O'Keefe J. Place navigation impaired in rats with hippocampal lesions. *Nature*. 1982;297:681–3.
32. Deacon RMJ, Rawlins JNP. T-maze alternation in the rodent. *Nat Protoc*. 2006;1:7–12.
33. Fouad S, Elfarrash S, Rizk A, Rezk S, Mosbah E, Saad MA et al. Cerebrolysin recovers diaphragmatic function and reduces injury-associated astrogliosis following a cervical spinal cord hemi-section injury in rats. *Egypt J Neurol Psychiatry Neurosurg*. 2023;59.
34. Livak KJ, Schmittgen TD. Analysis of relative gene expression data using real-time quantitative PCR and the 2- $\Delta\Delta C_T$  method. *Methods*. 2001;25:402–8.
35. Crowe A, Yue W. Semi-quantitative determination of protein expression using immunohistochemistry staining and analysis: an Integrated Protocol. *Bio-Protocol*. 2019;9.
36. Takeuchi H, Iba M, Inoue H, Higuchi M, Takao K, Tsukita K et al. P301S mutant human tau transgenic mice manifest early symptoms of human tauopathies with dementia and altered sensorimotor gating. *PLoS ONE*. 2011;6.
37. Brigas HC, Ribeiro M, Coelho JE, Gomes R, Gomez-Murcia V, Carvalho K et al. IL-17 triggers the onset of cognitive and synaptic deficits in early stages of Alzheimer's disease. *Cell Rep*. 2021;36.
38. Heikal SA, Fawi G, Moustafa SA, Barakat M, Ragab G, Hegazy MT et al. Serum Alpha-Synuclein and Inflammatory Markers prole in an Egyptian Alzheimer's and Parkinson's Diseases patients: A Pilot Study. 2024; <https://doi.org/10.21203/rs.3.rs-3893418/v1>.
39. Ransohoff RM. How neuroinflammation contributes to neurodegeneration. *Science (80-)*. 2016. p. 777–83.
40. Ferreira SA, Romero-Ramos M. Microglia response during Parkinson's disease: alpha-synuclein intervention. *Front Cell Neurosci*. 2018;12.
41. Haukedal H, Freude K. Implications of Microglia in Amyotrophic lateral sclerosis and Frontotemporal Dementia. *J Mol Biol*. 2019. p. 1818–29.
42. Guzman-Martinez L, Maccioni RB, Andrade V, Navarrete LP, Pastor MG, Ramos-Escobar N. Neuroinflammation as a common feature of neurodegenerative disorders. *Front Pharmacol*. 2019.
43. Parhizkar S, Holtzman DM. APOE mediated neuroinflammation and neurodegeneration in Alzheimer's disease. *Semin Immunol*. 2022.
44. Ramsey CP, Glass CA, Montgomery MB, Lindl KA, Ritson GP, Chia LA, et al. Expression of Nrf2 in neurodegenerative diseases. *J Neuropathol Exp Neurol*. 2007;66:75–85.
45. Rojo AI, Pajares M, Rada P, Nuñez A, Nevado-Holgado AJ, Killik R, et al. NRF2 deficiency replicates transcriptomic changes in Alzheimer's patients and worsens APP and TAU pathology. *Redox Biol*. 2017;13:444–51.
46. Zhang H, Davies KJA, Forman HJ. Oxidative stress response and Nrf2 signaling in aging. *Free Radic Biol Med*. 2015.
47. Yang Y, Jiang S, Yan J, Li Y, Xin Z, Lin Y et al. An overview of the molecular mechanisms and novel roles of Nrf2 in neurodegenerative disorders. *Cytokine Growth Factor Rev*. 2015.
48. Volonte D, Liu Z, Musille PM, Stoppani E, Wakabayashi N, Di YP et al. Inhibition of nuclear factor-erythroid 2-related factor (Nrf2) by caveolin-1 promotes stress-induced premature senescence. *Mol Biol Cell*. 2013.
49. Tarantini S, Valcarcel-Ares MN, Yabluchanskiy A, Tuscsek Z, Hertelendy P, Kiss T, et al. Nrf2 Deficiency exacerbates obesity-Induced oxidative stress, neurovascular dysfunction, blood-brain barrier disruption, Neuroinflammation, Amyloidogenic Gene expression, and Cognitive decline in mice, mimicking the aging phenotype. *Journals Gerontol - Ser Biol Sci Med Sci*. 2018;73:853–63.
50. Joshi G, Gan KA, Johnson DA, Johnson JA. Increased Alzheimer's disease-like pathology in the APP/PS1 $\delta$ E9 mouse model lacking Nrf2 through modulation of autophagy. *Neurobiol Aging*. 2015;36:664–79.
51. Syapin PJ. Regulation of haeme oxygenase-1 for treatment of neuroinflammation and brain disorders. *Br J Pharmacol*. 2008. p. 623–40.
52. Jazwa A, Cuadrado A. Targeting Heme Oxygenase-1 for Neuroprotection and Neuroinflammation in neurodegenerative diseases. *Curr Drug Targets*. 2012;11:1517–31.
53. Wong SY, Tan MGK, Wong PTH, Herr DR, Lai MKP. Andrographolide induces Nrf2 and heme oxygenase 1 in astrocytes by activating p38 MAPK and ERK. *J Neuroinflammation*. 2016;13.
54. Delaidelli A, Richner M, Jiang L, van der Laan A, Bergholdt Jul Christiansen I, Ferreira N et al.  $\alpha$ -Synuclein pathology in Parkinson disease activates homeostatic NRF2 anti-oxidant response. *Acta Neuropathol Commun*. 2021;9.
55. Yousef MH, Salama M, El-Fawal HAN, Abdelnaser A. Selective GSK3 $\beta$  inhibition mediates an Nrf2-Independent anti-inflammatory microglial response. *Mol Neurobiol*. 2022;59:5591–611.
56. Wang Y, Tian Y, Ding Y, Wang J, Yan S, Zhou L et al. MiR-152 may silence translation of camk ii and induce spontaneous immune tolerance in mouse liver transplantation. *PLoS ONE*. 2014;9.
57. Smith E, Stark MA, Zarbock A, Burcin TL, Bruce AC, Vaswani D, et al. IL-17A inhibits the expansion of IL-17A-Producing T cells in mice through short-Loop Inhibition via IL-17 receptor. *J Immunol*. 2008;181:1357–64.
58. Bolpetti A, Silva JS, Villa LL, Lepique AP. Interleukin-10 production by tumor infiltrating macrophages plays a role in human papillomavirus 16 tumor growth. *BMC Immunol*. 2010;11.
59. Dai Y, Zhang Z, Cao Y, Mehta JL, Li J. MiR-590-5p inhibits Oxidized-LDL Induced Angiogenesis by Targeting LOX-1. *Sci Rep*. 2016;6.

## Publisher's Note

Springer Nature remains neutral with regard to jurisdictional claims in published maps and institutional affiliations.